Photon Orbital Angular Momentum in Astrophysics

Martin Harwit

511 H St., SW, Washington, DC 20024; also Cornell University, harwit@verizon.net

Received _____; accepted _____

arXiv:astro-ph/0307430v1 24 Jul 2003

ABSTRACT

Astronomical observations of the *orbital angular momentum of photons*, a property of electromagnetic radiation that has come to the fore in recent years, have apparently never been attempted. Here, I show how measurements of this property of photons have a number of astrophysical applications.

Subject headings: Instrumentation: Miscellaneous – Masers – ISM: General – Extraterrestrial Intelligence – Black Hole Physics – Cosmology: Cosmic Microwave Background

1. Introduction

Photons are endowed with spin angular momentum $\pm\ \hbar$ along their direction of propagation. Beams of photons all carrying the same spin are circularly polarized. Less well known is that photons can also carry orbital angular momentum (OAM), ℓ, quantized in units of $\hbar$. Curtis, Koss & Grier (2002) have produced beams of photons each with OAM as high as $\ell = 200\ \hbar$,

Progress in laboratory studies of photon orbital angular momentum (POAM) has been rapid since Allen, Beijersbergen, Spreeuw & Woerdman (1992) first pointed out that laser — and by inference maser — modes with well-defined POAM can be readily produced. The characteristics of this radiation are by now reasonably well established (Allen, Padgett & Babiker, 1999; Allen, 2002).

A new development within the last year has been the introduction of a straightforward technique for measuring the OAM of individual photons (Leach et al, 2002). Rather than measuring the angular momentum of the photons directly, the new method sorts

photons according to their symmetry properties. This should permit the introduction of measurements of POAM into astronomy.

In section 2 of this paper, I provide a short quantitative introduction to POAM, followed in section 3 by a description of the astronomical instrumentation required to detect POAM and several of its limitations. Section 4 lists a range of astrophysical observations that could be undertaken. Section 5 briefly summarizes the findings.

2. Multipole Fields

Spherical electromagnetic waves in free space, like all waves entailing divergence-free fields, $\nabla \cdot \mathbf{E} = \nabla \cdot \mathbf{H} = 0$, can be completely described by superpositions of electric and magnetic multipole fields. For an electric multipole the magnetic field is transverse to the direction of propagation (TM mode), while for a magnetic multipole the electric field is transverse (TE mode). The TE and TM modes are dual to each other, related through the transforms

$$\mathrm{E}^{(E)} \rightarrow -\mathrm{H}^{(M)} \quad \text{and} \quad \mathrm{H}^{(E)} \rightarrow \mathrm{E}^{(M)} \tag{1}$$

where the superscripts (E) and (M) respectively indicate TE and TM modes (Rose, 1955). The two modes correspond to two orthogonal senses of polarization (Jackson, 1975, P 398).

Classically the angular momentum of an electromagnetic wave is given by the volume integral of the cross product of position $\mathbf{r}$ measured from the center of the multipole and the Poynting vector $\mathbf{S}$ at $\mathbf{r}$

$$\mathbf{J} = \frac{1}{c^2} \int \mathbf{r} \wedge \mathbf{S} dV = \frac{1}{4\pi c} \int \mathbf{r} \wedge (\mathbf{E} \wedge \mathbf{H}) dV \ . \tag{2}$$

The same expression holds in quantum electrodynamics, but the vector field strengths now become operators acting on a state vector Ψ. $\mathbf{J}$ can give rise to two components which

may not always be clearly separable, $\mathbf{J} = \mathbf{J_o} + \mathbf{J_s}$, respectively the orbital and spin angular momenta.[1]

Quantum mechanically, one writes

$$\mathbf{J} = -i\,\hbar\,\mathbf{r} \wedge \nabla \quad + \quad \hbar\,\mathbf{s}\ , \tag{3}$$

where $\mathbf{s}$ is the spin matrix for a vector field (Franz, 1950; Rose, 1955). The two angular momentum eigenvalue equations deriving from the angular momentum operator are

$$J_z\mathbf{E} = m\,\hbar\,\mathbf{E} \quad \text{and} \quad J^2\mathbf{E} = \ell(\ell+1)\,\hbar^2\,\mathbf{E}\ . \tag{4}$$

From (2) it is clear that only the radial components of $\mathbf{E}$ or $\mathbf{H}$ can contribute to the net angular momentum of a wave. For electric multipole radiation these components take the form (Heitler, 1936, 1954)

$$H_r = 0\ , \quad E_r = \frac{\mathcal{A}_\ell^m S(kr)}{r(kr)^{1/2}} e^{-i\omega t)} P_\ell^m(\cos\theta) e^{im\phi} \tag{5}$$

where $\mathcal{A}_\ell^m$ reflects the amplitude of the multipole, $S(kr)$ is derived from Bessel functions $J_{\ell+1/2}$, and P_ℓ^m is the associated Legendre polynomial. ℓ and m are integers with $|m| \leq \ell$. ω is the angular frequency and k the wave number. The multipole axis lies along some direction ϵ_z, to which the vector $\mathbf{r}$ is inclined at an angle θ, and ϕ is the azimuthal angle about the z-axis.

Classically, a vibrational motion along the multipole axis radiates perpendicular to this axis, while a rotation about the z-axis produces radiation with angular momentum directed along the multipole axis. (Morette De Witt & Jensen, 1953). [2] Quantum mechanically,

---

[1]For different views on this separability and its dependence on gauge invariance, see Jauch & Rohrlich (1955), P40; Gottfried (1966), page 412; Allen, Padgett & Babiker (1999), p 304.

[2]For further discussions, see Heitler (1954), Gottfried (1966), and Jackson (1975). The

the z-component of the first term in (3) can be written as $J_z = -i\,\hbar\,\delta/\delta\phi$ (Jackson, 1975, P 743), showing that the term $e^{im\phi}$ in equation (5) gives rise to an angular momentum component m about the z-axis. In contrast, the spin component of the angular momentum in (3) is Lorentz invariant, always takes on the value $\pm\,\hbar$, and is directed along the axis of propagation.

The propagating electromagnetic wave consists of m intertwined helical wave fronts, and m is called the *winding number* or *topological charge*. All phases ϕ appear along the beam axis, $r = 0$, and the resulting destructive interference leads to zero intensity there. Constructive interference occurs at some radius r_m off the beam axis, so that light brought to a focus forms a ring of radius

$$r_m = \frac{a\lambda f}{\pi\rho}\left(1 + \frac{m}{m_0}\right)\ , \tag{6}$$

and width comparable to the wavelength λ. Here f the focal length, ρ the radius of the optical train's effective aperture, and the values $a \sim 2.585$ and $m_0 \sim 9.80$ are experimentally determined (Curtis & Grier, 2003). In the limit of low values of m the ring has dimensions small compared to the Airy disk.

Barnett and Allen (1994) examined the general relationship between energy and angular momentum along the direction of propagation for electromagnetic radiation and obtained the expression

$$\frac{J_z}{\mathcal{E}} = \frac{(m+\sigma)}{\omega} + \frac{\sigma}{\omega}[g(k)]. \tag{7}$$

$g(k) << 1$ reflects the spectral and spatial distribution of the radiation, and tends to be

---

contemporary literature on POAM, concerned largely with laser optics, uses the symbol ℓ for the magnetic quantum number m. This is at variance with the earlier literature and customary usage in physics. I have tried to avoid confusion by adhering to the notation of the three cited books.

negligibly small.

From (7) we see that though the spin and orbital angular momenta cannot be cleanly separated, it is always possible to measure the orbital angular momentum by passing a beam through a linear polarizer, which sets $\sigma = 0$, and leaves the orbital angular momentum intact. The ratio $J_z/\mathcal{E}$ then is m/ω.

3. Astronomical Instrumentation to Measure POAM

3.1. Dove-Prism Mach-Zehnder Interferometers

With a relatively simple experiment, He et al (1995) were the first to show that POAM can be transferred to small particles. Working with a linearly polarized helium-neon laser beam that could be switched between m values $+3$ and -3 they set finely divided CuO grains suspended in water into clockwise or counterclockwise rotation, at will.

Experiments by O'Neil et al. (2002) and Curtis & Grier (2003) have clearly shown that the angular momentum absorbed by such small particles is orbital angular momentum, rather than spin. They trapped microscopic particles in the highly focused annular image of radius r_m produced by a laser beam with POAM $m = 40$. The particles then circled the optical axis along this annulus.

Until recently, however, there was no straightforward method for measuring the OAM of a single photon with unknown m. The provision of such a method now opens up for astronomy a technique that should prove itself valuable.

The method has been described by Leach et al. (2002). Their apparatus was designed to deal with laser-generated modes, but the procedure is general though instrumental details will differ for different wavelength ranges and applications. The method does not directly

measure POAM. Instead, it identifies the symmetry properties of a beam of electromagnetic radiation subjected to a sequence of rotations about its axis of propagation. This is achieved by sending light through a cascade of Mach-Zehnder interferometers with Dove prisms in each arm (Fig. 1). At each stage the beams in the two interferometer arms are rotated with respect to one another through an angle α, where $\alpha/2$ is the relative rotation of the Dove prisms about the optical axis in each beam. The first interferometer stage has $\alpha/2 = \pi/2$ and sorts photons with even values of orbital angular momentum m into one exit port and those with odd values of m into the other port. The photons with odd values of m are then sent through a hologram (Fig. 2(b)) that increases the POAM m carried by each photon to a value $m + 1$, thus endowing all the photons with even values of m.

Each of the beams emerging from the two ports of this first stage is then sent through a second Mach-Zehnder stage of its own, in which the two Dove prisms are rotated by an angle $\alpha/2 = \pi/4$ relative to each other. These two stages, respectively dedicated to what originally were odd and even modes m, now separate modes with $m = 4n$, where n is an integer, from those with $m = 4n + 2$. This process is continued in successive Mach-Zehnder stages until photons with all desired values of m have been sieved out. Leach et al., (2002) have demonstrated that the method provides clean separation for individual photons with m = 0, 1, 2, and 3 when passed through a two-stage apparatus. In principle, the Dove prisms could be replaced by equivalent all-reflective elements for use over wide wavelength ranges.

The winding number m is invariant under a Lorentz transformation. This makes it a robust indicator of the orbital angular momentum.

3.2. Astronomical Limitations

The theory discussed thus far can be applied to the detection of radiation from individual atoms, molecules or lasers. However, use of the technique of Leach et al. (2002) requires rotating a beam with multipole characteristics (ℓ, m) around the multipole symmetry axis z. The angular distribution of the radiation about this axis is (Blatt & Weisskopf, 1952, page 594)

$$\Omega_\ell^m(\theta,\phi) = \frac{1}{2}\left[1 - \frac{m(m+1)}{\ell(\ell+1)}\right]|Y_\ell^{m+1}|^2 + \frac{1}{2}\left[1 - \frac{m(m-1)}{\ell(\ell+1)}\right]|Y_\ell^{m-1}|^2 + \frac{m^2}{\ell(\ell+1)}|Y_\ell^m|^2 \quad (8)$$

where the normalized spherical harmonics are

$$Y_\ell^m(\theta,\phi) = \left[\frac{2\ell+1}{4\pi}\frac{(\ell-|m|)!}{(\ell+|m|)!}\right]^{1/2} P_\ell^m(\cos\theta)e^{im\phi} \ . \quad (9)$$

Equation (8) holds for pure modes. A superposition of modes can lead to interference effects affecting the angular distribution.

The associated Legendre polynomials P_ℓ^m have a deep null along the multipole axis for all quantum numbers $m \neq 0$, irrespective of ℓ. This means that astronomical radiation incident on a telescope is extremely weak near the multipole axis unless $m = 0$ or, alternatively, the beam is highly collimated, as for masers, and a helical structure is imposed on the beam through an azimuthal phase shift. This limitation appears to be universal, and extends to other means for determining POAM.

4. Astrophysical Applications

Despite these limitations a number of astrophysical applications emerge.

4.1. Masers as Probes of Inhomogeneities

Observations by Bignall et al. (2003) dramatically illustrate the existence of large density inhomogeneities in the interstellar medium on small scales. They observed radio flux density changes of up to 40%, over a period as short as 45 minutes, from the quasar PKS 1257-326. Interstellar and circumstellar masers similarly tend to be associated with shocked domains. To reach Earth, the radiation traverses regions that may well have discontinuities impressing OAM on transmitted electromagnetic waves. These effects can be sizeable because the refractive index n of the interstellar medium is substantial. The group velocity of the wave is $c/n = c[1 + \omega_p^2/\omega^2]^{-1/2}$, where ω is the angular frequency of the wave and $\omega_p \sim 5.6 \times 10^4 n_e^{1/2}$ rad s^{-1} is the plasma frequency. For a cosmic-ray-induced ionization fraction $n_e/n_H \sim 10^{-6}$, a delay of one wavelength is reached over a distance of

$$D \sim 10^{12} \left(\frac{10^{-5}}{n_e/n_H}\right) \left(\frac{10^5 \text{ cm}^{-3}}{n_H}\right) \left(\frac{20 \text{ cm}}{\lambda}\right) \text{ cm} , \tag{10}$$

which is small compared to the dimensions of the turbulent region around an evolved star, where masers are typically found at radial distances 10^{16} to 10^{17} cm. A turbulent screen with significant density spikes, through and around which the maser beam has to pass, is therefore likely to induce POAM.

To visualize the production of POAM by a maser beam passing through an inhomogeneous medium, one can envision the beam illuminating a spiral phase plate (Fig. 2(a)). The top surface of the plate is displaced by a height s after a full azimuthal rotation $\phi = 2\pi$. At a radial distance r from the optical axis the local azimuthal slope of this surface is $\theta = s/2\pi r$. On emerging from the phase plate a ray passing through r is deflected by an angle Ψ, where Snell's law for small angles gives $(\Psi + \theta) \sim n\theta$, and n is the refractive index of the plate. It is easy to see that $\Psi \sim (n-1)\theta = (n-1)s/2\pi r$.

Before entering the spiral phase plate, a photon's linear momentum is h/λ. On

exiting the phase plate, the component of the photon's linear momentum in the azimuthal direction is $p_\phi \sim h\Psi/\lambda$, and its angular momentum about the optical axis is $J_z = rp_\phi \sim rh\Psi/\lambda \sim (n-1)\ \hbar\ /s\lambda = m\ \hbar$. Here the step height s is chosen an integer multiple m of $\lambda/(n-1)$, so that $s = m\lambda/(n-1)$. J_z is independent of the radial distance r at which radiation passes through the phase plate.

A turbulent medium with discontinuities can be envisaged as a screen of such spiral phase plates. The analysis of spatial discontinuities may then entail tracking changes in the observed winding number for individual circumstellar masers as the turbulent supersonic outflow from the parent star progresses.

4.2. Luminous Point Sources

Radiation emitted by luminous pulsars and quasars may also encounter density discontinuities in traversing the immediate surroundings of these respective sources (cf. Zavala & Taylor, 2003). These discontinuities again can impose a twist on the radiation, similar to that produced by a spiral phase plate or a holographic phase plate. Here, as in the example of the maser cited above, the axis of propagation reaching the telescope is defined by the line of sight from the source to the telescope, and the discontinuity inducing the POAM lies along this line of sight. The effective multipole axis is, therefore, collinear with the axis of propagation, and measurement of the POAM is feasible.

An earmark of discontinuities in a plasma is that $J_z \propto (n-1)/\lambda \propto \omega_p^2/\omega$ for a phase plate with step height s. Since $\mathcal{E} \propto \omega$ this means that $J_z/\mathcal{E} \propto \omega^{-2}$ and by (7) $m \propto \omega^{-1} \propto \lambda$.

4.3. SETI

A number of investigators have recently turned to visual wavelengths in their Search for Extraterrestrial Intelligence, SETI. This comes at a time when researchers in optical communication have discovered significant advantages that radiation with high values of POAM might have for communication and quantum computing. The ability to encode a single photon with $\log_2 N$ bits of information, by endowing it with a POAM of $N\,\hbar$ in place of the conventional single bit of information granted by photon spin, carries great promise while also providing possibilities for entanglement (Vaziri, Weihs & Zeilinger, 2002). For SETI an additional advantage would be the absence of naturally occurring optical photons with high POAM. Artificially generated photons would thus be more readily culled out from naturally occurring diffuse optical radiation in space.

In order to measure the POAM of a SETI transmission, the observer will again need to gather radiation surrounding the multipole axis of the propagating beam. This may be achieved with arrays of telescopes both at the transmitting and receiving ends, in order to keep the beam sufficiently narrow. For a separation D between transmitters and receivers operating at a wavelength λ the array baseline d would have to be $d \sim 170(\lambda D)^{1/2}$ km, where λ is measured in microns and D in parsecs. For planets the size of the Earth, this should permit access over distances of order a hundred parsecs. At the receiving end, the incoming radiation would be directed to a central station where it could be rotated around its multipole axis, as in the method of Leach et al. (2002). O'Neil et al. (2002) have studied the case where the optical axis of the beam is not precisely centered on the receiving optics. The orbital angular momentum density is affected, but the winding number should remain unaltered.

4.4. Transfer of OAM by Kerr Black Holes

Teukolsky (1972) first looked in detail at the interaction of electromagnetic radiation with Kerr black holes. Mashhoon (1973) soon thereafter pointed out that electromagnetic radiation scattered off black holes would absorb some of the hole's angular momentum. More recently Falcke, Melia & Agol (2000) have discussed observations to detect the shape of a dark shadow in the immediate vicinity of a rapidly rotating black hole. To date, however, the transfer of angular momentum to POAM has not been discussed.

Angular momentum transfer and gravitational lensing of electromagnetic radiation both are wavelength independent. Angular momentum transfer from a Kerr black hole might be expected to induce a helical form on an incident wave, just as a phase plate does, except that the angle Ψ in Fig. 1 would be independent of wavelength. More specifically, radiation from a distant unresolved source incident on a Kerr black hole along its axis of symmetry and lensed by the hole should leave the right side of equation (7) independent of wavelength and exhibit orbital angular momentum m proportional to ω or, equivalently, λ^{-1}. A full theoretical investigation of such effects would be of interest as a guide to searches in MACHO surveys.

4.5. Blackbody Radiation and the Cosmic Microwave Background

A question that arises is how the existence of an additional set of well defined OAM quantum states could be compatible with the conventional partition function encountered in blackbody radiation, $Z(\nu)d\nu = (8\pi\nu^2 d\nu/h^3)$, for radiation frequency ν in interval $d\nu$ and unit volume.

We may consider isolating a narrow bandwidth of radiation emanating from a blackbody source, selecting a fine pencil of this radiation and passing this through a linear

polarizer, before permitting it to enter the cascade of Dove-Prism Mach-Zehnder stages introduced by Leach et al. (2002). Knowing the width of the pencil beam, the bandwidth and the polarization, permits calculation of $Z(\nu)d\nu$. By providing additional information about the quantum number m, the cascade of Leach et al. (2002) would then appear to endow the radiation with more degrees of freedom than the partition function permits, in apparent violation of Bose-Einstein statistics and the Heisenberg uncertainty principle.

The error in this conclusion is that measurement of the photon orbital angular momentum introduces a calculable uncertainty in the direction of the Poynting vector, which corkscrews around the axis of propagation and thus introduces an uncertainty in the lateral momentum. As the experiment of Curtis & Grier illustrates, radiation no longer focuses onto a point, but rather onto a ring. In the limit of high m equation (6) makes clear that the circumference of the ring, i.e. the uncertainty in the lateral momentum increases linearly with m. Whatever information we can gain about an individual photon's orbital angular momentum corresponds to an identical loss of information about its direction of propagation.

Blackbody radiation is a superposition of multipole fields of many orders, ℓ, and we should expect this to be true of the cosmic microwave background radiation, CMBR. [3] Our line of sight to the surface of last scattering intersects this surface at right angles, so the radiation reaching us will have been emitted perpendicular to this surface, i.e. along the multipole axis. Equation (8), however, shows that only radiation characterized by Legendre polynomials of form P_ℓ^0 are emitted along the multipole axis, and we should expect all the received radiation to exhibit quantum number $m = 0$, corresponding to different values of

[3]It is important to note that we are here dealing with the multipole structure of the electric and magnetic field components, rather than the more frequently encountered multipole expressions for the CMBR surface brightness distribution.

ℓ, mutually interfering and indistinguishable. This yields the correct partition function.

If the multipole distribution of m values, measured by the probability distribution $P(m)$ were to be found to significantly differ from $m = 0$ along some lines of sight to the CMBR, we could gain information about discontinuities along those sight lines, as discussed in section 5. Gravitational discontinuities would produce a dependence of winding number $m \propto \omega$, distinguishing these from density discontinuities, for example in shocked regions of intracluster plasma, which would exhibit $m \propto \omega^{-1}$.

5. Conclusion

Astronomical observations to detect photon orbital angular momentum appear to have never been undertaken to date. I have cited a few astrophysical observations that might be attempted to gain new insight into different observational phenomena, and have listed several of the problems facing the measurement of POAM. Further theoretical as well as observational efforts will be required to clarify the unfamiliar interaction of POAM with matter, gravitation and magnetic fields.

Acknowledgments

I am greatly indebted to Prof. Les Allen for his incisive and helpful critique of this paper. I also thank Peter Nisenson, Harvey Moseley and Emil Wolf for their comments on an earlier version of the manuscript. Conversations with David Grier, Richard Lyon, Alex Kutyrev, John Mather, Harvey Moseley, Jürgen Stutzki and Edward Wollack were helpful and instructive. My work in infrared astronomy has been supported by contracts from NASA.

Figure Captions

Fig. 1. First stage of a Dove-Prism Mach-Zehnder interferometer cascade for sorting photons carrying different amounts of orbital angular momentum (after Leach et al., 2002).

Fig. 2. Photon orbital angular momentum (POAM) produced by a spiral phase plate (a), and an example of a holographic phase plate (b) (after Allen et al., 1999). For details see the text.

References

Abel, T., Bryan, G. L., & Norman, M. L. 2002, Science, 295, 93

Allen, L., Beijersbergen, M. W., Spreeuw, R. J. C. & Woerdman, J. P. 1992, Phys. Rev. A, 45, 8185

Allen, L., & Padgett, M. J. 200, Opt. Commun., 184, 67

Allen, L., Padgett, M. J., & Babiker, M. 1999, Progress in Optics, XXXIX, 291

Allen, L. 2002, J. Opt. B: Quantum Semiclass. Opt., 4, S1

Barnett, S. M., & Allen, L. 1994, Opt. Comm., 110, 670

Bignall H. E. et al. 2002, ApJ, 585, 653

Blatt, J. M. & Weisskopf, V. F. 1952, *Theoretical Nuclear Physics*, Wiley, New York

Curtis, J. E., & Grier, D. G. 2003, PRL, 133901

Curtis, J. E., Koss, B.A., & Grier, D. G. 2002, Opt. Commun., 207, 169

Falcke, H. Melia, F. & Agol, E. 2000, ApJ, 528, L13

Franz, W. 1950, Zeitschrift f. Physik, 126, 363

Fuller, T. M. & Couchman, H. M. P. 2000, ApJ, 544, 6.

Gottfried, K. 1966, *Quantum Mechanics, Volume 1, Fundamentals*, Benjamin/Cummings

He, H., Friese, M. E. J., Heckenberg, N. R., & Rubinsztein-Dunlop, H. 1995, PRL, 75, 826

Heitler, W. 1936, Proc. Camb. Phil. Soc., 32, 112

Heitler, W. 1954, *The Quantum Theory of Radiation* 3rd edition, Oxford, pages 401-4

Jackson, J. D. 1975, *Classical Electrodynamics*, John Wiley & Sons, New York, Chapter 16

Jauch, J. M., & Rohrlich, F. 1955, Addison-Wesley, Reading

Leach, J. Padgett, M. J., Barnett, S. M., Franke-Arnold, S. & Courtial, J. 2002, PRL, 88, 257901

Mashoon, B. 1973, Phys. Rev., D 7, 2807

Morette De Witt, C. & Jensen, J. H. D. 1953, Z. f. Naturforschung, 8a, 267

O'Neil, A. T., Mac Vicar, I., Allen, L. & Padgett, M. J. 2002, PRL, 88, 053601

Rose, M. E. 1955, *Multipole Fields*, John Wiley & Sons, New York

Teukolsky, S. A. 1972, PRL, 29, 1114

Vaziri, A., Weihs, G. & Zeilinger, A. 2002, PRL, 89, 240401

Zavala, R. T. & Taylor, G. B. 2003, ApJ, 589, 126

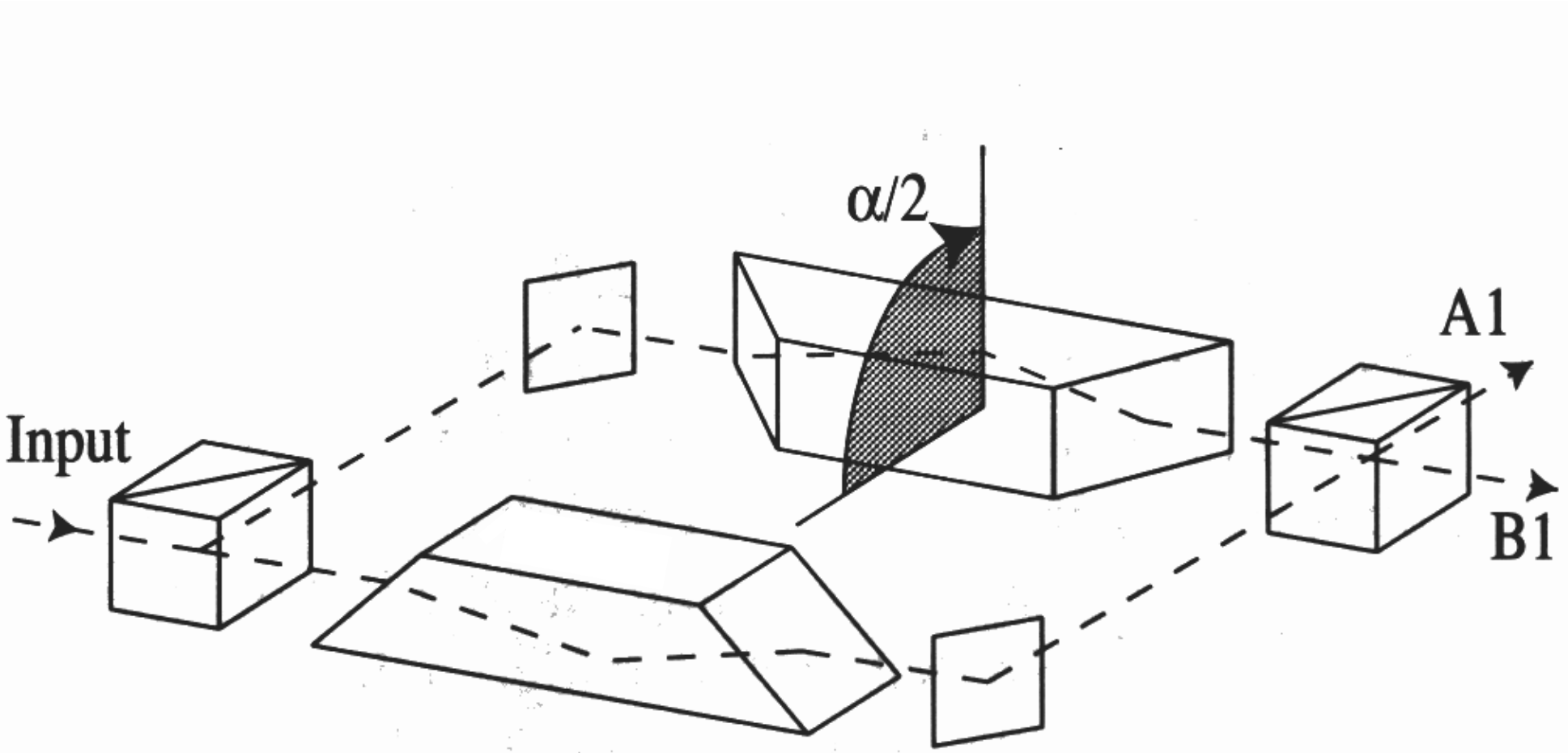
α/2
A1
Input
B1

(a)

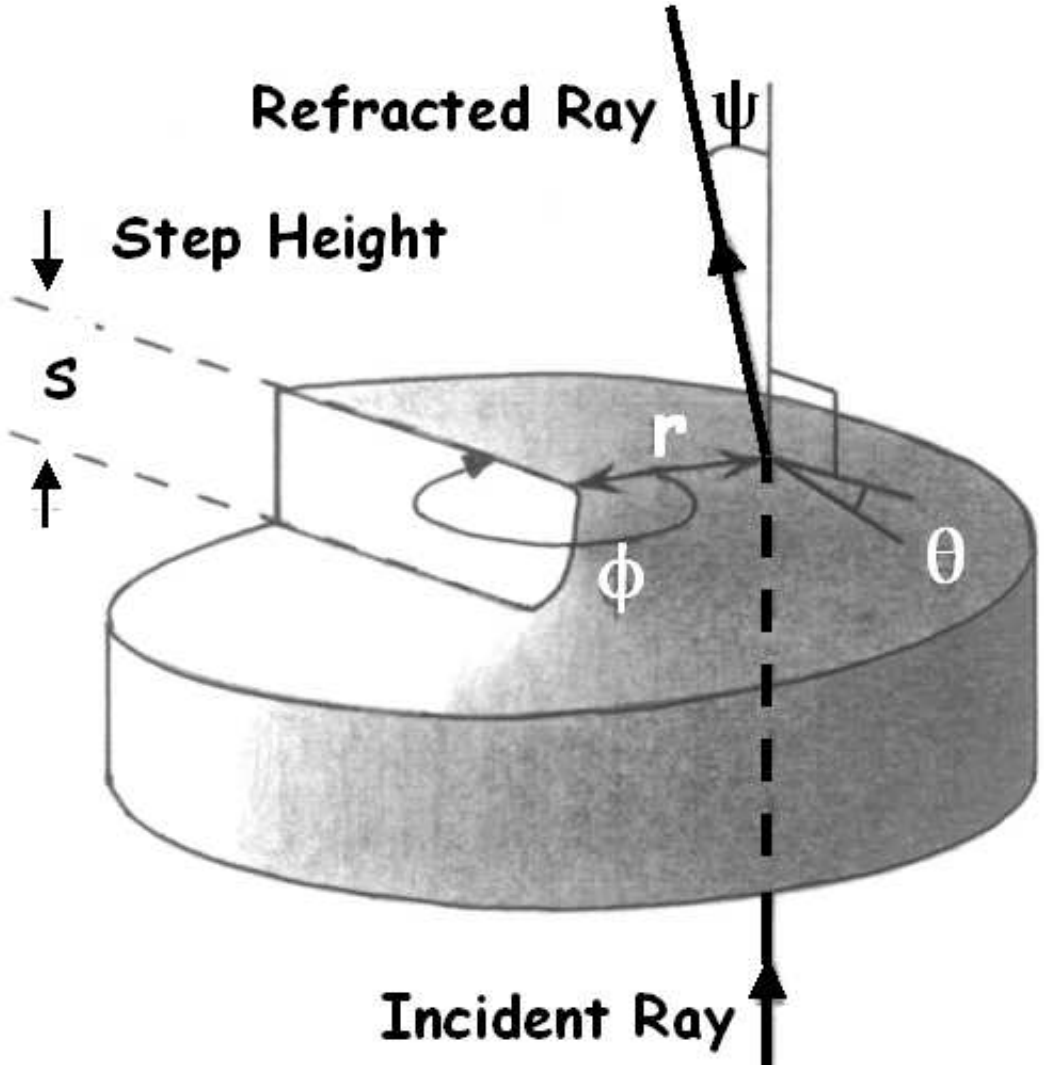

(b)